SEMARAK ILMU PUBLISHING

Journal of Advanced Research in Micro and Nano Engineering

Journal homepage:
https://semarakilmu.com.my/journals/index.php/micro_nano_engineering/index
ISSN: 2756-8210

Three-Dimensional Model of Ionic Species Concentration and Flux During Localised Corrosion of Steel in Marine Environment

Suhaila Salleh[1,2,*], Noor Mirza Syamimi Mortadha[3], Ariff Alzakri[4]

[1] Fakulti Teknologi dan Kejuruteraan Mekanikal, Universiti Teknikal Malaysia Melaka, Hang Tuah Jaya, 76100 Durian Tunggal, Melaka, Malaysia
[2] Centre for Advanced Research on Energy, Universiti Teknikal Malaysia Melaka, Hang Tuah Jaya, 76100 Durian Tunggal, Melaka, Malaysia
[3] Department of Mechanical and Manufacturing Technology, Kolej Vokasional Datuk Seri Mohd Zin, 78000 Alor Gajah, Melaka, Malaysia
[4] School of Engineering, University of Edinburgh, Edinburgh EH9 3FB, United Kingdom

ARTICLE INFO

Article history:
Received 1 August 2024
Received in revised form 25 September 2024
Accepted 28 October 2024
Available online 30 November 2024

Keywords:
Model; corrosion; steel

ABSTRACT

Localized corrosion, exemplified by pitting and crevice corrosion, presents a significant challenge in industrial and marine settings due to the presence of chloride ions in seawater, brines and industrial fluids. It initiates and spreads at specific points on metal surfaces and its hidden rapid metal degradation beneath intact surface layers complicates detection and monitoring, increasing the risk of unforeseen structural failures and jeopardizing critical infrastructure integrity. Factors influencing its severity include chloride concentration, pH levels, temperature variations and aggressive ion presence, which degrade protective oxide layers and expose metal to accelerated corrosion. This study aims to enhance predictive capabilities to effectively manage corrosion in chloride-rich environments. Using COMSOL Multiphysics software, this study models a microscale geometry representing a micropit and simulates chloride-induced localized corrosion in steel, by integrating Nernst-Planck equations to incorporate electrochemical reactions, ion transport dynamics and three-dimensional geometrical features. Key parameters such as chloride concentration, pH and material properties are crucial in the modelling approach to simulate the formation and growth of corrosion sites. For 0 to 800 seconds simulation, the model displays the flux of ionic species into and out of the pit. At 800 second, the results demonstrate a peak of Fe^{2+} concentration of approximately 2.53×10^3 mol/m^3 at the deepest section, the Cl^- of 7×10^3 mol/m^3 and an increase in H^+ inside the pit, reducing the pH from 8 to about 4.9. These concentration changes indicate substantial metal dissolution is actively occurring inside the pit, making COMSOL Multiphysics software a versatile platform for coupling multiphysical phenomena, enabling comprehensive analysis and 3D visualization of corrosion processes.

1. Introduction

Corrosion science represents a vital area of research and application, crucial for understanding and managing the degradation of steel structures due to environmental factors. Steel, renowned for its strength and versatility, plays a pivotal role in numerous industries, including construction,

* *Corresponding author.*
E-mail address: suhaila@utem.edu.my

https://doi.org/10.37934/armne.25.1.2738

infrastructure and manufacturing. However, its susceptibility to corrosion when exposed to moisture, oxygen and aggressive chemicals necessitates a deep understanding of the underlying mechanisms. Localised corrosion, specifically in the form of pitting and crevice corrosion, represents a persistent and significant challenge in the utilization of steel and other metallic materials in various industrial and marine environments [1-3]. This type of corrosion occurs when chloride ions, often present in seawater, brines, de-icing salts or industrial process fluids, create aggressive local environments that initiate and propagate corrosion at specific points on the metal surface. Unlike uniform corrosion, which affects the entire exposed surface evenly, localised corrosion can lead to rapid and localized material degradation, potentially causing catastrophic failures even in structurally sound components. The detrimental effects of localised corrosion are exacerbated by its insidious nature, often occurring beneath intact surface layers where corrosion is not readily visible. This makes detection and monitoring challenging, increasing the risk of unexpected structural failures. Moreover, localised corrosion can compromise the integrity of critical infrastructure such as pipelines, offshore platforms, bridges and chemical processing equipment, leading to safety hazards, environmental risks and substantial economic losses [4,5].

The severity of localised corrosion is influenced by various factors including chloride concentration, pH levels, temperature, oxygen availability and the presence of aggressive ions or contaminants [6]. These factors contribute to the breakdown of protective oxide layers (passive films) on steel surfaces, exposing fresh metal to corrosive attack. Once initiated, corrosion pits or crevices can act as preferential sites for ongoing degradation, progressing even under conditions where the surrounding metal remains relatively unaffected.

Efforts to mitigate localised corrosion typically involve materials selection, protective coatings, corrosion inhibitors and improved design practices tailored to specific environmental conditions. However, these approaches require a thorough understanding of the underlying corrosion mechanisms and the ability to predict corrosion behaviour under realistic operational scenarios [7].

In this context, ongoing research focuses on advanced modelling and simulation techniques to simulate the complex interactions between chloride ions, steel surfaces and environmental factors [8-10]. These efforts aim to enhance predictive capabilities, optimize corrosion management strategies and ultimately prolong the service life of steel structures exposed to chloride-rich environments. This introduction sets the stage for exploring the nuances of localised corrosion of steel with chloride and underscores the importance of addressing this persistent challenge through interdisciplinary research and innovative engineering solutions.

One of the key challenges with localized corrosion is its covert nature, often occurring beneath intact surface layers where corrosion is not immediately visible. This characteristic makes detection and monitoring difficult, heightening the risk of unexpected structural failures. Critical infrastructure like pipelines, offshore platforms, bridges and chemical processing equipment are particularly vulnerable, posing safety hazards, environmental risks and substantial economic losses if compromised.

This interdisciplinary field integrates principles from electrochemistry, materials science and engineering to elucidate the complex processes leading to corrosion initiation and propagation in steel. Modelling localized corrosion is crucial for understanding these complex processes that occur at microscopic scales [11], influencing the degradation of metals in various environments [12,13]. Localized corrosion phenomena such as pitting and crevice corrosion are influenced by multiple factors including environmental conditions [14], material properties [15] and electrochemical reactions [16]. These processes are particularly exacerbated by chloride ions in marine environments and industrial settings, leading to accelerated material loss and structural integrity issues.

From the science of corrosion, it is found that pitting or crevice corrosion, occurs when chloride ions penetrate the protective oxide layer on metal surfaces, initiating aggressive chemical reactions in localized areas despite the surrounding metal remaining relatively intact [1]. The initiation and propagation of chloride-induced localized corrosion are influenced by multiple factors including environmental conditions (e.g., temperature, humidity), alloy composition, surface defects and the presence of other ions. Understanding these complex interactions is crucial for developing effective corrosion mitigation strategies and designing corrosion-resistant materials. Besides advanced techniques such as electrochemical impedance spectroscopy (EIS) and scanning electron microscopy (SEM), computational modelling has indeed provided deeper insights into the mechanisms governing chloride-induced pitting corrosion.

There exist a number of software applications that have been developed to tackle multiphysics engineering challenges, yielding robust observations and results essential for analysing real-world engineering issues [17,18]. COMSOL Multiphysics represents cutting-edge software capable of addressing both multiphysics and multiscale problems, empowering researchers to construct intricate computational models that incorporate multiple physical processes. This software provides a versatile platform for designing, optimizing and predicting the behaviour of systems and devices under different conditions.

Corrosion science has extensively employed modelling techniques, often validated against published research [19]. However, the exact mechanisms governing the initiation of pits on metal surfaces remain incompletely understood despite numerous studies [20,21]. Researchers have developed both a two-dimensional axisymmetric model [22] and a three-dimensional model [23] to investigate the propagation of pits after their initial stages. Several factors affect the corrosion rate of steel in sodium chloride solutions, including chloride ion concentration, solution pH, temperature and the presence of contaminants [8]. Recently, studies have shown that steel immersed in mildly alkaline chloride solutions can clarify localized corrosion phenomena, particularly pitting [22,23]. In this study, the aim is to create a three-dimensional model of a single microscale pit that represents an active pit after the initiation stage. Using COMSOL Multiphysics software, the model is set with the initial pH of the surrounding immersion liquid slightly alkaline at pH 8. Through the corrosion model, the goal is to produce polarization curves that illustrate the relationship between current density and electrode potential across varying initial pH values and display the flux of ionic species into and out of the pit geometry. These curves will predict the evolution of the corroding metal surface under different potential conditions.

2. Methodology

2.1 Geometrical Model of Corrosion

The corrosion geometry model was developed in COMSOL Multiphysics software. The design of the corrosion structure was constructed with two parts which were the bulk solution and the corroding pit. Figure 1 shows the geometry of the model used to simulate this project. The model features a box-shaped domain (Domain 1) representing the bulk solution outside the metal, while the pit (Domain 2) represents the corroding metal itself. The lower part of the pit (Domain 2) has dimensions of $1x10^{-6}$ meter (m) in radius and a depth of $1x10^{-7}$ m. The active area below the box-shaped region facilitates interactions between ionic species and the surrounding environment, defining where all reactions occur within the specified pH and potential conditions.

Domain 1 serves to simulate the immersing solution, with the pit mouth facilitating migration processes both into and out of the pit. This region is electrically insulated in the software, with no

current flow predefined. In contrast, Domain 2 is configured as active, representing the area where metal dissolution takes place.

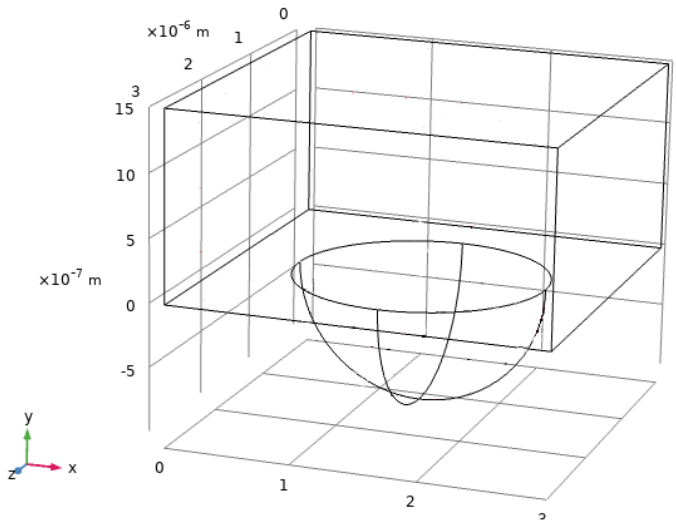

Fig. 1. Corrosion geometrical model

The total current inflow, i_{tot} of the model, adheres to the following governing rule as in Eq. (1) below:

$$i_{tot} = (J_{diss} - J_{H^+}) \times F \tag{1}$$

where the Faraday's constant, *F* (96485 C/mol), rate of iron oxidation/dissolution, J_{diss}, rate of proton reduction, J_{H^+}, respectively.

The dissolved iron has generated a flux, which is reflected in the activity expression denoted by J_{diss}. Similarly, for Fe^{2+}, the boundary condition was established based on flux. This correlation is linked to the reduction in H^+ concentration, where the activity expression follows $-J_{H^+}$, with H^+ also set as flux at the boundary condition.

2.2 Nernst-Planck Equation

The Nernst-Planck equations are extensively employed in scientific literature to model the movement of ionic species in electrochemical systems [24]. They represent a physical reformulation of Fick's macroscopic diffusion law, incorporating the motion of charged particles. The equation was originally proposed by Nernst, who experimentally validated its principles and theoretically developed by Planck [25]. COMSOL has the capability to incorporate the Nernst-Planck equations in scenarios where electroneutrality is both maintained and not maintained. By opting to enforce electroneutrality universally, a more resilient model can be established. In this framework, the movement of each species in the solution adheres to the principles of the Nernst-Planck law under conditions where electroneutrality is rigorously applied, as shown in Eq. (2) below.

$$\frac{\partial [i]}{\partial t} = D_i \nabla^2 [i] + z_i U_i F \nabla([i] \nabla V) + R_i \tag{2}$$

where the concentration of species *i,* $[i]$, the effective diffusion coefficient, D_i, charge number, z_i, mobility, U_i (given that U_i=$\frac{Di}{RT}$), rate of production/depletion of *i,* R_i, potential gradient, ∇V respectively.

2.3 Ionic Species

This model has eleven species which react in the aqueous alkaline solution, namely:

i. Metal ion from dissolution process (Fe^{2+}).
ii. Hydroxyl ion (OH^-).
iii. Hydrogen ion (H^+).
iv. Iron (II) monohydroxide ion ($FeOH^+$).
v. Sodium ion (Na^+).
vi. Chloride ion (Cl^-).
vii. Iron (II) chloride ion ($FeCl^+$).
viii. Metal ions (Fe^{3+}).
ix. Iron (III) dioxide ion (FeO_2^-).
x. Iron hydroxide oxide ion ($HFeO_2^-$).
xi. Iron (III) dichloride ion ($FeCl_2^+$).

This model considered the diffusion, electromigration and chemical reaction.

3. Results

This section discusses the results obtained when the model was simulated for potential -1.0 to -0.2 V which is equivalent to simulation time of 800 seconds.

3.1 Ionic Concentration Distribution Inside the Pit
3.1.1 Concentration of Fe^{2+}

Figure 2 presents a three-dimensional model depicting the concentration of Fe^{2+} ions at pH8 across various times: 200 s, 400 s, 700 s and 800 s. The concentration of Fe^{2+} inside the pit reaches a peak value of 2.53×10^3 mol/m^3, which is higher than at the pit mouth, consistent with findings by Salleh *et al*., [20,21]. This active region exhibits significant Fe^{2+} dissolution, indicative of ongoing corrosion processes within this area. The accumulation of Fe^{2+} ions inside the pit necessitates balancing with negatively charged ionic species to maintain electro-neutrality in the solution. Additionally, the model shows Fe^{2+} ions beginning to accumulate in the upper region of the pit, aligning with diffusion theory where species move from areas of high concentration to low concentration until equilibrium is achieved across the system.

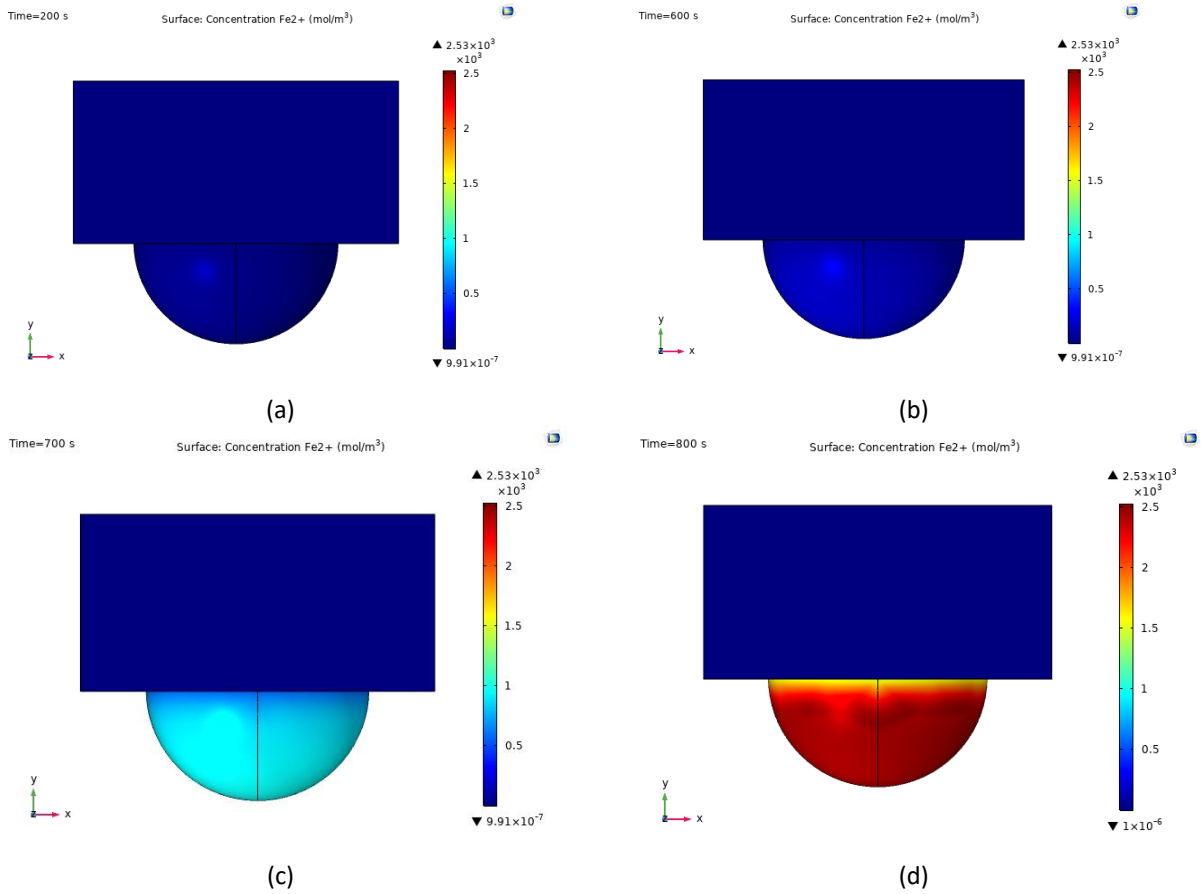

Fig. 2. Concentration of Fe^{2+} at time (a) 200 s (b) 600 s (c) 700 s (d) 800 s

3.1.2 Concentration of Cl^-

Figure 3 depicts the Cl^- concentration at pH 8 within the pit at the conclusion of the simulation, specifically at 800 s. The Cl^- concentration begins to rise at -0.4 V potential around 600 s and continues increasing until -0.2V. As shown in Figure 2, the Fe^{2+} concentration is notably elevated in the pit region, indicating substantial metal dissolution, particularly in the pit's lowermost section. The Cl^- concentration model below illustrates a concentration level of 7×10^3 mol/m^3 inside the pit, underscoring active metal dissolution at the modelled boundary's lowest point, which is designated as an active area in the model.

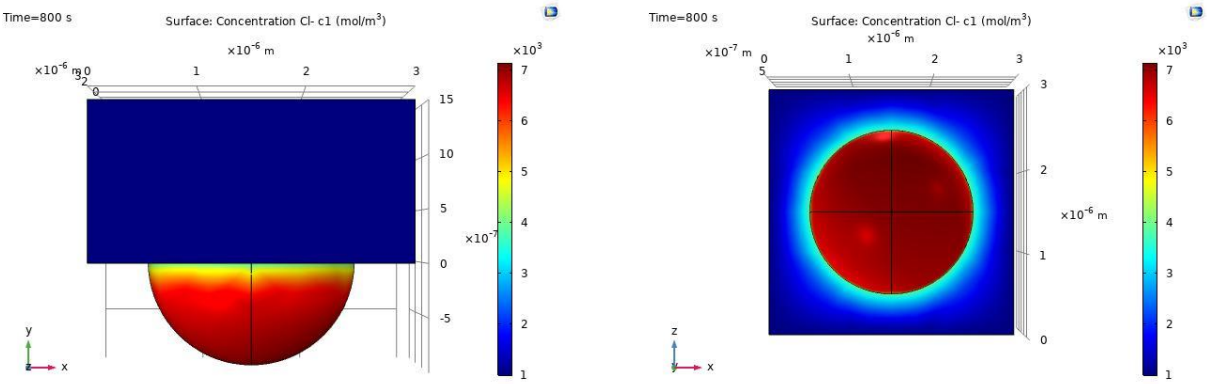

Fig. 3. Concentration Cl^- at 800 s

3.1.3 Concentration of H^+

Figure 4 presents the H^+ concentration inside the pit at 800s within a pH 8 environment. The H^+ concentration starts increasing around -0.6 V potential and continues to rise until -0.2 V. The increase in H^+ concentration results from the hydrolysis reaction between Fe^{2+} and water. This process leads to acidification of the pit environment, as documented in the study by Lee *et al.,* [26] and supported by model studies conducted by Mousson *et al.,* [27].

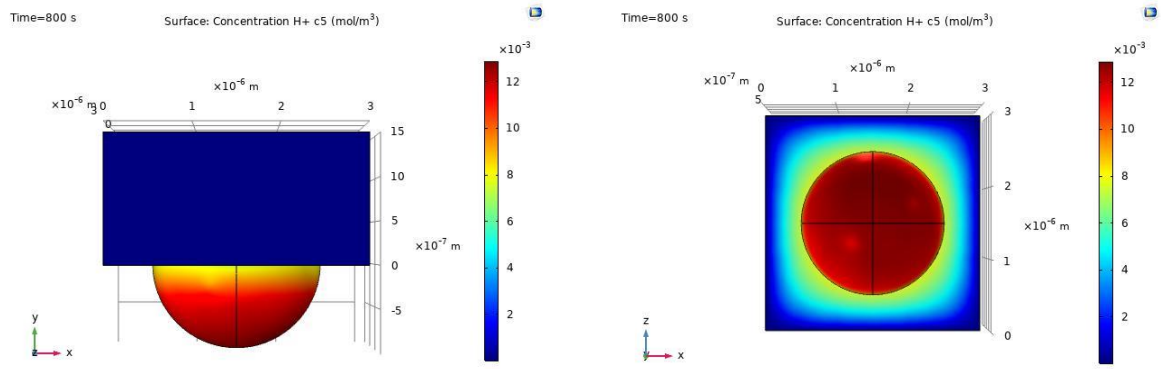

Fig. 4. Concentration of H^+ at 800 s

3.2 pH Change

Figure 5 displays a plotted graph depicting the pH values at Point 6 (a point at the bottom of the pit) and Point 5 (a point at the mouth of the pit) against potential. The graph illustrates a decrease in pH as the potential becomes more anodic. At -1.0 V potential, both points show a pH slightly above 8. At this potential, the concentration of OH^- exceeds that of H^+ due to the depletion of H^+ by the hydrogen evolution reaction. However, as the potential increases further, this effect diminishes. Within the pit, the pH remains at 8 under mild cathodic potentials and starts decreasing when the potential reaches -0.6 V due to the Fe^{2+} hydrolysis process. At -0.5 V potential, a pH lower than 5 was observed inside the pit, which is within acceptable limits as stated by Pourbaix and L'Hostis [28] for local corrosion of steel. The pH reduction is attributed to the hydrolysis process, which lowers the pH to below 5. The acidity of the environment increases with higher concentrations of hydrogen ions, as demonstrated in experiments [26]. Figure 4 illustrates ion concentrations, showing a significant increase in H^+ concentration starting from -0.6 V potential. This rapid decrease in pH, from 8 to below 5 starting at -0.6 V, aligns with findings by Salleh [22], who reported a pH solution result of 4.7. The pH at the bottom of the pit was observed to be more acidic compared to the area at the pit mouth.

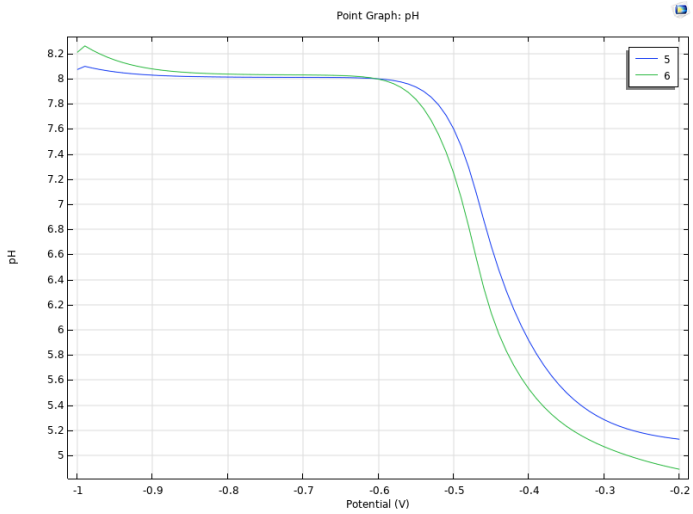

Fig. 5. Graph of pH vs potential

Figure 6 depicts the three-dimensional corrosion model in a pH 8 environment at 800s, corresponding to a potential of -0.2V. The model is color-coded to represent the pH values across different regions. In the inactive upper region of the geometry, the pH remains constant at 8 under this potential. However, in the active lower part, which forms the pit shape, the pH drops to 4.9, indicating an acidic environment. This decrease is directly correlated with the increased concentration of H^+, as illustrated in Figure 4 above. The pH dynamics are governed by the hydrolysis of Fe^{2+} with water, a process that leads to an accumulation of H^+ ions, thereby altering the alkalinity of the pit environment. The presence of H^+ ions attract Cl^- ions into the pit, where they combine to form hydrochloric acid, further contributing to the acidic nature and lowering the pH of the surrounding region.

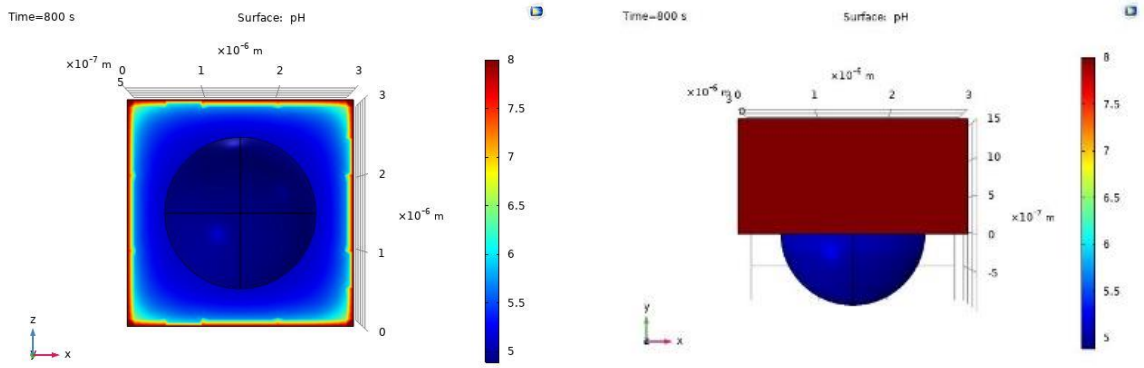

Fig. 6. Illustration of three-dimensional model for pH at 800 s

3.3 Flux of Ionic Species

Figure 7 to Figure 9 depict the total flux of ionic species H^+, Fe^{2+} and Cl^- at 800 s during the modelling process. Arrows indicate the direction of flux movement for each ionic species. Specifically, the arrows for H^+ and Fe^{2+} ions show movement out of the pit, while Cl^- flux arrows move towards the pit region. The dissolution of Fe^{2+} inside the pit represents the anodic reaction. A significant concentration of H^+ ions move out of the pit region due to its anodic nature, where electrons released by the anode flow towards the cathode, facilitating their outward movement. The accumulation of positive metal ions within the pit creates a local excess of positive charge, attracting Cl^- ions from the

electrolyte into the pit through migration to maintain charge neutrality. Theoretically, the pit contains a high concentration of $FeCl^+$, a product of the electrochemical reaction between Fe^{2+} and Cl^-, which increases in response to Fe^{2+} concentration. At anodic potentials, Fe^{2+} undergoes hydrolysis to produce $FeOH^+$ and H^+ ions. The increasing concentration of H^+ leads to acidification of the surrounding environment, causing a decrease in pH of the solution and turning the environment acidic.

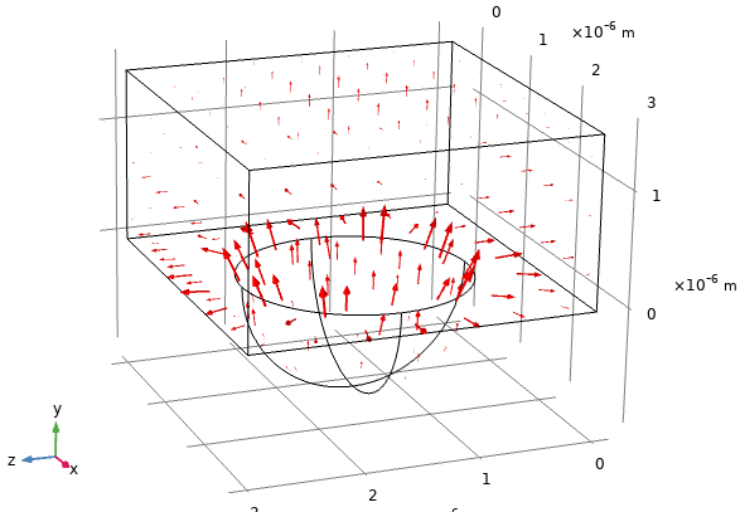

Fig. 7. Total flux of H^+ species

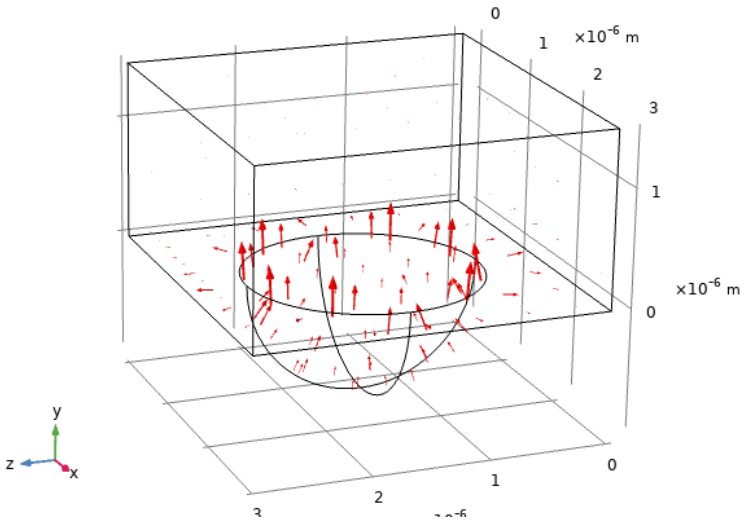

Fig. 8. Total flux of Fe^{2+} species

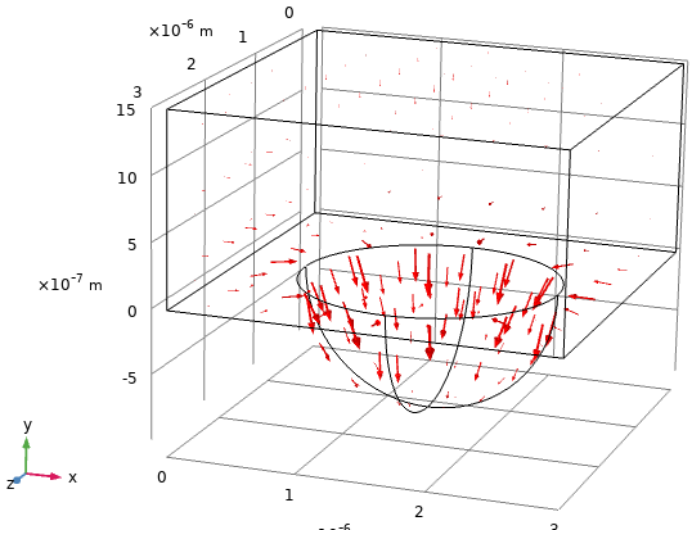

Fig. 9. Total flux of Cl^- species

3.4 Summary

The corrosion process involves intricate interactions among ionic species, characterized by their diffusion and migration. A model was employed to vividly portray these dynamics across defined ranges of potential and time, offering insights into how these species traverse into and out of corroding pits, thereby generating notable concentration gradients and shifts in ionic compositions.

Throughout the observation period, simultaneous alterations in the concentrations of all species were meticulously tracked. Notably, an uptick in Fe^{2+} concentration served as a direct indicator of metal depletion from the surface. The model effectively visualized these transformations, presenting concentration profiles for each species in relation to varying potentials. Moreover, it underscored distinct concentration disparities between specific locations within the corroding pit, such as at its mouth versus its bottom.

Utilizing comprehensive data on species concentrations vis-à-vis potential, the model enabled precise calculations of corrosion rates under specific environmental conditions or temporal intervals. Remarkably, it disclosed that the dissolution rate of metal was notably higher at the pit's base compared to its entrance.

The progression of potential was correlated with elapsed time, unveiling temporal dependencies in the corrosion phenomena. Furthermore, the model elucidated a significant environmental shift within the pit itself: despite an initial ambient pH of 8, the pH inside the pit gradually dwindled to 4.9. This acidic milieu, distinctly confined to the pit, stemmed from the chemical reaction between hydrogen ions (H^+) and chloride ions (Cl^-), culminating in the production of hydrochloric acid (HCl).

In summary, through its meticulous depiction of ionic movements, concentration gradients and environmental transformations, the model not only deepened our understanding of corrosion processes but also provided crucial insights into how localized chemical environments evolve within corroding structures.

4. Conclusions

In conclusion, the three-dimensional model has successfully displayed the migration and diffusion of ionic species into and out of the corroding pit. The simulation highlights a significant peak of Fe^{2+} concentration of approximately 2.53×10^3 mol/m^3 at the deepest section of the geometrical pit, along with an increase in Cl^- concentration of 7×10^3 mol/m^3 within the pit from potential -0.4V until -0.2V,

taking 600 seconds. A significant drop of pH from 8 to 4.9 inside the pit is an observation resulting from the formation of hydrochloric acid from accumulation of H^+ and Cl^-. These concentration and pH changes indicating substantial metal dissolution and corrosion activities. This underscores the ongoing process of metal dissolution at the lowest boundary of the three-dimensional modelled pit, emphasizing the dynamic interplay of electrochemical processes and environmental factors.

Acknowledgement
This research was funded by a grant from the Ministry of Higher Education of Malaysia (FRGS Grant, No: FRGS/1/2018/STG06/UTEM/02/2). The authors would also like to thank Universiti Teknikal Malaysia Melaka (UTeM) for all the support given.

References

[1] Sharland, S. M. "A review of the theoretical modelling of crevice and pitting corrosion." *Corrosion science* 27, no. 3 (1987): 289-323. https://doi.org/10.1016/0010-938X(87)90024-2
[2] Alamri, Aeshah H. "Localized corrosion and mitigation approach of steel materials used in oil and gas pipelines–An overview." *Engineering failure analysis* 116 (2020): 104735. https://doi.org/10.1016/j.engfailanal.2020.104735
[3] Arzaghi, Ehsan, Bing H. Chia, Mohammad M. Abaei, Rouzbeh Abbassi and Vikram Garaniya. "Pitting corrosion modelling of X80 steel utilized in offshore petroleum pipelines." *Process Safety and Environmental Protection* 141 (2020): 135-139. https://doi.org/10.1016/j.psep.2020.05.024
[4] Ezuber, Hosni M., Abdulla Alshater, SM Zakir Hossain and Ali El-Basir. "Impact of soil characteristics and moisture content on the corrosion of underground steel pipelines." *Arabian Journal for Science and Engineering* 46 (2021): 6177-6188. https://doi.org/10.1007/s13369-020-04887-8
[5] Wasim, Muhammad, Shahrukh Shoaib, N. M. Mubarak, Inamuddin and Abdullah M. Asiri. "Factors influencing corrosion of metal pipes in soils." *Environmental Chemistry Letters* 16 (2018): 861-879. https://doi.org/10.1007/s10311-018-0731-x
[6] Song, Yarong, Guangming Jiang, Ying Chen, Peng Zhao and Yimei Tian. "Effects of chloride ions on corrosion of ductile iron and carbon steel in soil environments." *Scientific reports* 7, no. 1 (2017): 6865. https://doi.org/10.1038/s41598-017-07245-1
[7] Cai, Yikun, Yuanming Xu, Yu Zhao and Xiaobing Ma. "Atmospheric corrosion prediction: a review." *Corrosion Reviews* 38, no. 4 (2020): 299-321. https://doi.org/10.1515/corrrev-2019-0100
[8] Feng, Weipeng, Anel Tarakbay, Shazim Ali Memon, Waiching Tang and Hongzhi Cui. "Methods of accelerating chloride-induced corrosion in steel-reinforced concrete: A comparative review." *Construction and Building Materials* 289 (2021): 123165. https://doi.org/10.1016/j.conbuildmat.2021.123165
[9] Trávníček, Pavel, Tomáš Koudelka, Jaroslav Kruis, Šárka Msallamová and Jiří Němeček. "A new model for chloride ion diffusion in cracked concrete with consideration of damage and strain fields." *Construction and Building Materials* 438 (2024): 136920. https://doi.org/10.1016/j.conbuildmat.2024.136920
[10] Yu, Qifeng and Tongyan Pan. "Microstructural Modeling of Pitting Corrosion in Steels Using an Arbitrary Lagrangian–Eulerian Method." *Metallurgical and Materials Transactions A* 48 (2017): 2618-2632. https://doi.org/10.1007/s11661-017-4018-9
[11] Guo, Peng, Erika Callagon La Plante, Bu Wang, Xin Chen, Magdalena Balonis, Mathieu Bauchy and Gaurav Sant. "Direct observation of pitting corrosion evolutions on carbon steel surfaces at the nano-to-micro-scales." *Scientific reports* 8, no. 1 (2018): 7990. https://doi.org/10.1038/s41598-018-26340-5
[12] Si, Wujun, Qingyu Yang and Xin Wu. "Material degradation modeling and failure prediction using microstructure images." *Technometrics* (2019). https://doi.org/10.1080/00401706.2018.1514327
[13] Jafarzadeh, Siavash, Jiangming Zhao, Mahmoud Shakouri and Florin Bobaru. "A peridynamic model for crevice corrosion damage." *Electrochimica Acta* 401 (2022): 139512. https://doi.org/10.1016/j.electacta.2021.139512
[14] Kim, Changkyu, Lin Chen, Hui Wang and Homero Castaneda. "Global and local parameters for characterizing and modeling external corrosion in underground coated steel pipelines: A review of critical factors." *Journal of Pipeline Science and Engineering* 1, no. 1 (2021): 17-35. https://doi.org/10.1016/j.jpse.2021.01.010
[15] Brewick, Patrick and Andrew Geltmacher. "Investigating How Microstructural Features Influence Stress Intensities in Pitting Corrosion." In *Challenges in Mechanics of Time Dependent Materials, Fracture, Fatigue, Failure and Damage Evolution, Volume 2: Proceedings of the 2019 Annual Conference on Experimental and Applied Mechanics*, pp. 77-85. Springer International Publishing, 2020. https://doi.org/10.1007/978-3-030-29986-6_12

[16] Ansari, Talha Qasim, Jing-Li Luo and San-Qiang Shi. "Modeling the effect of insoluble corrosion products on pitting corrosion kinetics of metals." *npj Materials Degradation* 3, no. 1 (2019): 28. https://doi.org/10.1038/s41529-019-0090-5

[17] Bryant, Daniel John Ebrahim and K. C. Ng. "Numerical modelling of hydraulic jump using mesh-based cfd method and its comparison with lagrangian moving-grid approach." *Journal of Advanced Research in Micro and Nano Engineering* 10, no. 1 (2022): 1-6.

[18] Elfaghi, Abdulhafid MA, Alhadi A. Abosbaia, Munir FA Alkbir and Abdoulhdi AB Omran. "CFD Simulation of Forced Convection Heat Transfer Enhancement in Pipe Using Al2O3/Water Nanofluid." *Journal of Advanced Research in Micro and Nano Engineering* 7, no. 1 (2022): 8-13. https://doi.org/10.37934/cfdl.14.9.118124

[19] Jafarzadeh, Siavash, Ziguang Chen and Florin Bobaru. "Computational modeling of pitting corrosion." *Corrosion reviews* 37, no. 5 (2019): 419-439. https://doi.org/10.1515/corrrev-2019-0049

[20] Brenna andrea, Fabio Bolzoni, Luciano Lazzari and Marco Ormellese. "Predicting the risk of pitting corrosion initiation of stainless steels using a Markov chain model." *Materials and Corrosion* 69, no. 3 (2018): 348-357. https://doi.org/10.1002/maco.201709753

[21] Li, Xuanpeng, Yang Zhao, Wenlong Qi, Jidong Wang, Junfeng Xie, Hairui Wang, Limin Chang et al. "Modeling of pitting corrosion damage based on electrochemical and statistical methods." *Journal of The Electrochemical Society* 166, no. 15 (2019): C539. https://doi.org/10.1149/2.0401915jes

[22] Salleh, Suhaila. *Modelling pitting corrosion in carbon steel materials*. The University of Manchester (United Kingdom), 2013.

[23] Salleh, Suhaila, Noor Mirza Syamimi Mortadha and Alzakri Ekhwan. "Polarization Curve of Chloride-Induced Corrosion in Steel Using a Three-Dimensional Model." *Journal of Advanced Research in Applied Mechanics* 106, no. 1 (2023): 27-36. https://doi.org/10.37934/aram.106.1.2736

[24] Metti, Maximilian S., Jinchao Xu and Chun Liu. "Energetically stable discretizations for charge transport and electrokinetic models." *Journal of Computational Physics* 306 (2016): 1-18. https://doi.org/10.1016/j.jcp.2015.10.053

[25] Maexa, Reinoud. "Nernst-planck equation." In *Encyclopedia of computational neuroscience*, pp. 2182-2187. New York, NY: Springer New York, 2022. https://doi.org/10.1007/978-1-0716-1006-0_233

[26] Lee, Y. H., Z. Takehara and S. Yoshizawa. "The enrichment of hydrogen and chloride ions in the crevice corrosion of steels." *Corrosion Science* 21, no. 5 (1981): 391-397. https://doi.org/10.1016/0010-938X(81)90075-5

[27] Mousson, Jean-Louis, Bruno Vuillemin, Roland Oltra, Didier Crusset, Gerard Santarini and Pierre Combrade. "Modeling of the propagation of crevice corrosion." (2004).

[28] Pourbaix, A. and V. L'Hostis. "Passivation, localised corrosion and general corrosion of steel in concrete and bentonite. Theory and experimentals." In *Journal de Physique IV (Proceedings)*, vol. 136, pp. 71-78. EDP sciences, 2006. https://doi.org/10.1051/jp4:2006136008